The International Journal of Biochemistry & Cell Biology 55 (2014) 119–128

Contents lists available at ScienceDirect

The International Journal of Biochemistry & Cell Biology

journal homepage: www.elsevier.com/locate/biocel

The phospholipase D pathway mediates the inflammatory response of the retinal pigment epithelium

Melina V. Mateos*, Constanza B. Kamerbeek, Norma M. Giusto, Gabriela A. Salvador*

Instituto de Investigaciones Bioquímicas de Bahía Blanca (INIBIBB), Universidad Nacional del Sur (UNS) and Consejo Nacional de Investigaciones Científicas y Técnicas (CONICET), Edificio E1, Camino La Carrindanga km 7, 8000 Bahía Blanca, Argentina

ARTICLE INFO

Article history:
Received 9 June 2014
Received in revised form 12 August 2014
Accepted 18 August 2014
Available online 27 August 2014

Keywords:
ARPE-19 cells
Retinal pigment epithelium (RPE)
Inflammation
Phospholipase D (PLD)
Cyclooxygenase-2

ABSTRACT

The retinal pigment epithelium (RPE) plays an important immunological role in the retina and it is involved in many ocular inflammatory diseases that may end in loss of vision and blindness. In this work the role of phospholipase D (PLD) classical isoforms, PLD1 and PLD2, in the inflammatory response of human RPE cells (ARPE-19) was studied.

ARPE-19 cells exposed to lipopolysaccharide (LPS, 10 μg/ml) displayed increased levels of NO production and diminished mitochondrial function after 48 h of incubation. Furthermore, 24 h LPS treatment strongly induced cyclooxygenase-2 (COX-2) expression and activation of extracellular signal-regulated kinase (ERK1/2). EGFP-PLDs showed the typical subcellular localization, perinuclear for PLD1 and plasma membrane for PLD2. LPS increased PLD activity by 90% with respect to the control. The presence of PLD1 inhibitor (EVJ 0.15 μM) or PLD2 inhibitor (APV 0.5 μM) reduced LPS-induced COX-2 induction but only PLD2 inhibition reduced ERK1/2 activation. Mitochondrial function was restored after inhibition of PLD2 and ERK1/2. These findings evidence the participation of PLD2 as a promoter of RPE inflammatory response through ERK1/2 and COX-2 regulation. Our results demonstrate for the first time distinctive roles of PLD isoforms in pathological conditions in RPE.

1. Introduction

The retinal pigment epithelium (RPE) is located between vessels of the choriocapillaris and the light-sensitive retina layer, and closely interacts with photoreceptors (PR) in the process of vision. RPE cells are essential for the maintenance of a healthy retina, and any impairment of their functionality may have deleterious effects on vital activities such as phagocytosis of PR rod outer segments or maintenance of the blood retinal barrier (Lamb et al., 2007; Strauss, 2005). Analyses of hereditary types of retinal degeneration disclose a strong dependence of PR on RPE cells. In line with this, mutations in genes which are expressed in RPE are responsible for primary PR degeneration (Sparrow et al., 2010). Increasing knowledge on the multiple functions performed by the RPE has contributed to the understanding of many diseases leading to blindness, such as Stargardt's disease (STGD), retinitis pigmentosa (RP) and age-related macular degeneration (AMD). RPE cells also mediate the immune response in the eye and can (Perez et al., 2013; Ishida et al., 2003) secrete immune modulatory factors, such as interleukin-8 (IL-8), complement factor H (CFH) or monocyte chemotactic protein-1 (MCP1) (Strauss, 2005).

In spite of the close homology of RPE with immune system cells, phospholipase D (PLD) expression and their role in this specialized epithelium remain unknown. PLD isoforms have been shown to be involved in many functions of the blood immune response. PLD catalyzes phosphatidylcholine (PC) hydrolysis to generate the lipid second messenger, phosphatidic acid (PA), and choline. PA generated by PLD can be further hydrolyzed by lipid phosphate phosphatases (LPPs) in order to generate diacylglycerol (DAG), another lipid second messenger (Peng and Frohman, 2012). The two most studied isoforms, PLD1 and PLD2, and their product, PA, have been involved in a variety of signaling and membrane

Abbreviations: AA, arachidonic acid; AMD, age-related macular degeneration; COX, cyclooxygenase; DAG, diacylglycerol; DR, diabetic retinopathy; EGFP, enhanced green fluorescent protein; ERK, extracellular signal-regulated kinase; EtOH, ethanol; HRP, horseradish peroxidase; iNOS, inducible nitric oxide synthase; LDH, lactate dehydrogenase; LPS, lipopolysaccharide; LPPs, lipid phosphate phosphatases; MAPKs, mitogen-activated protein kinases; MEK, MAPK kinase; NO, nitric oxide; OA, oleic acid; PA, phosphatidic acid; PC, phosphatidylcholine; PEth, phosphatidylethanol; PGs, prostaglandins; PIP_2-PLC, phosphatidylinositol bisphosphate-phospholipase C; PLD, phospholipase D; PR, photoreceptor; PVDF, polyvinylidene fluoride; RPE, retinal pigment epithelium; RP, retinitis pigmentosa; STGD, Stargardt's disease; TTBS, Tween-tris buffer solution.

* Corresponding authors. Tel.: +54 291 4861201; fax: +54 291 4861200.
E-mail addresses: mvmateos@criba.edu.ar, melinavaleriamateos@gmail.com (M.V. Mateos), salvador@criba.edu.ar (G.A. Salvador).

http://dx.doi.org/10.1016/j.biocel.2014.08.016
1357-2725/

trafficking events in different immunity cells (Jenkins and Frohman, 2005; McDermott et al., 2004; Zeng et al., 2009; Peng and Frohman, 2012).

RPE inflammatory processes are known to be associated with the above-mentioned pathologies. Prostaglandins (PGs) are the most important lipid mediators involved in the generation of the inflammatory response. They are generated from arachidonic acid (AA) by cyclooxygenase 2 (COX-2) action and their biosynthesis is significantly increased in inflamed tissue, thus contributing to the development of acute inflammation. COX-2 regulation involves gene transcriptional and post-transcriptional events, such as COX-2 mRNA stability and translational efficiency, specific microRNAs and RNA-binding proteins, and COX-2 alternative polyadenylation (Dixon et al., 2013). However, the intracellular signaling pathways involved in the regulation of COX-2 activity remain obscure.

Several lines of evidence described a functional role for PLD in COX-2 regulation during cell activation (He et al., 2008; Ahn et al., 2007; Kim et al., 2004). However, the contribution of PLD to COX-2 expression, posttranslational regulation and PGs production during inflammatory processes in the RPE has not yet been elucidated. Based on all these evidences, we tested the hypothesis of PLD participation in RPE inflammatory process. Specifically, we explored the crosstalk between PLD-generated signaling and COX-2 regulation in human retinal epithelium cells (ARPE-19). To this end, ARPE-19 cells were challenged with increasing lipopolysaccharide (LPS) concentrations (as an inflammatory model) and the activity, expression, subcellular localization of PLD1 and PLD2 isoforms and their involvement in COX-2 regulation and PGs production were analyzed.

2. Materials and methods

2.1. Reagents

Triton X-100, dimethyl sulfoxide (DMSO), U0126, U73122, Celecoxib, LPS from *Pseudomona aeruginosa* (L7018) and 3-(4,5-dimethylthiazol-2-yl)-2,5-diphenyltetrazolium bromide (MTT) were obtained from Sigma-Aldrich (St. Louis, MO, USA). VU0359595 or EVJ, VU0285655-1 or APV, oleic acid (OA) and arachidonic acid (AA) were from Avanti Polar Lipids, Inc. (Alabaster, AL, USA). Radiolabeled oleic acid [9,10-^{3}H(*N*)] ([^{3}H]-OA) (15–60 Ci/mmol) and arachidonic acid [5,6,8,9,11,12,14,15-^{3}H(*N*)] ([^{3}H]-AA) (60–100 Ci/mmol) were purchased from New England Nuclear-Dupont, Boston, MA, USA. Preblended dry fluor 2a70 (98% PPO and 2% bis-MSB) was obtained from Research Products International Corp. (Mount Prospect, IL, USA). All other chemicals were of the highest purity available.

2.2. Antibodies

Rabbit polyclonal antibodies anti-ERK1/2 (#9102), anti-phospho-ERK1/2 (#9101), and anti-PLD1 (#3832) were from Cell Signaling (Beverly, MA, USA). Rabbit polyclonal antibodies anti-TLR4 (H-80) (sc-10741) and anti-CD14 (M-305) (sc-9150), goat polyclonal anti-PLD2 antibody (sc-48269), polyclonal horse radish peroxidase (HRP)-conjugated goat anti-rabbit IgG and polyclonal HRP-conjugated goat anti-mouse IgG were purchased from Santa Cruz Biotechnology, Inc. (Santa Cruz, CA, USA). Mouse monoclonal anti-α Tubulin (DM1-A) (CP06) was from EMD/Biosciences-Calbiochem (San Diego, CA, USA). Rabbit polyclonal antibody anti-COX-2 (160116) and mouse monoclonal antibody anti-COX-1 (160110) were from Cayman Chemical (Ann Arbor, MI, USA). Mouse monoclonal antibody anti-EGFP (MMS-108P) was from Covance Inc. (Santa Cruz, CA, USA).

2.3. Retinal-pigmented epithelium cell culture and treatments

Human retinal-pigmented epithelium cells (ARPE-19) from the American Type Culture Collection (ATCC, Manassas, VA) were generously donated by Dr. E. Politi and Dr. N. Rotstein (INIBIBB, Bahía Blanca, Argentina). ARPE-19 cells, a spontaneously arising human RPE cell line, were routinely passaged by dissociation in 0.25% trypsin and 5 mM EDTA in Hanks' balanced salt solution without calcium and magnesium (HBSS), followed by replating at a split ratio 1:3. Cells were maintained in Dulbecco's Modified Eagle's Medium (DMEM) supplemented with 10% fetal bovine serum (FBS, Natocor, Argentina), 100 U/ml penicillin, 100 μg/ml streptomycin and 0.25 μg/ml amphotericin B at 37 °C under 5% CO_2. Confluent ARPE-19 cell cultures were serum-starved for 2 h prior to stimulation and treated for 2, 24, 48 or 72 h with different doses (5, 10 or 100 μg/ml) of *P. aeruginosa* LPS in serum-free DMEM. In control conditions the same volume LPS was replaced for sterile ultra pure water. Inhibition of specific signaling pathways was achieved by incubation of ARPE-19 cells with selective inhibitors for 1 h at 37 °C prior to cell stimulation with LPS. DMSO (vehicle of the inhibitors) was added to all conditions (including control conditions) to achieve a final concentration of 0.025%.

2.4. MTT reduction assay

MTT, a water-soluble tetrazolium salt, is reduced by metabolically viable cells to a colored, water-insoluble formazan salt. This reduction depends on the activity of mitochondrial dehydrogenases. After LPS treatment (for 24, 48 or 72 h), MTT (5 mg/ml, prepared in phosphate buffer saline) was added to the cell culture medium at a final concentration of 0.5 mg/ml. The culture dishes (35 mm) were incubated for 1 h at 37 °C in a 5% CO_2 atmosphere, cells were washed twice with phosphate buffer saline (PBS) and lysed with 600 μl of a buffer containing 10% Triton X-100 and 0.1 N HCl in isopropanol. The extent of MTT reduction was measured spectrophotometrically at 570 nm using a V-630 spectrophotometer (JASCO, Analytical Instruments). Results are expressed as arbitrary units with respect to the control condition.

2.5. LDH assay

Lactate dehydrogenase (LDH) leakage was evaluated as a parameter of plasma membrane integrity using kit LDH-P UV AA (Wiener laboratory, Rosario, Argentina). After LPS treatment (for 24, 48 and 72 h) LDH activity was measured spectrophotometrically in 50 μl of the culture medium following the manufacturer's instructions. Briefly, the rate of conversion of reduced nicotinamide adenine dinucleotide (NADH) to oxidized nicotinamide adenine dinucleotide (NAD^+) was followed at 340 nm using a V-630 spectrophotometer (JASCO Analytical Instruments).

2.6. Determination of NO production

Nitrites (NO_2^-) were measured in the incubation media as a stable and non-volatile breakdown product of the nitric oxide (NO) released by ARPE-19 cells, employing the spectrometric Griess reaction as previously described (Cutini et al., 2012).

2.7. COX-2 activity assay

To determine COX-2 activity, the generation of PGs F and E (PGF_2 and PGE_2) was measured. Confluent 60 mm dishes (2 per condition) were incubated at 37 °C with [^{3}H]-AA. The labeled fatty acid was mixed with unlabeled AA (final concentration of 1.5 μM and 0.25 μCi/dish) in the presence of lipid-free bovine serum albumin (BSA) (4 mol AA/mol BSA) in serum-free DMEM. Cells were

incubated with this medium for 24 h at 37 °C to allow [^{3}H]-AA incorporation. After 24 h, the medium was removed, the cells were washed three times with PBS and serum-free DMEM was added. Cells were then treated with LPS (10 μg/ml) or ultra pure water (control condition) for 24 h. When the effect of PLDs or ERK pathway on PGs production was studied cells were preincubated with the specific inhibitors for 1 h at 37 °C prior to cell stimulation with LPS. After stimulation, the medium was removed and PGs were then extracted, separated and quantified as described before (Rodriguez et al., 2012).

2.8. PLD activity assay

To assay PLD activity, transphosphatidylation reaction was measured in ARPE-19 cells treated with LPS or under control conditions. Confluent 35 mm dishes were incubated at 37 °C with [^{3}H]-OA. The labeled fatty acid was mixed with unlabeled OA (final concentration of 2.2 μM and 0.5 μCi/dish) in the presence of lipid-free bovine serum albumin (BSA) (4 mol OA/mol BSA) in serum-free DMEM. Cells were incubated with this medium for 24 h at 37 °C to allow [^{3}H]-OA incorporation. After 24 h, the medium was removed, cells were washed three times with PBS and serum-free DMEM was added. Cells were subsequently treated with LPS (10 μg/ml) or ultra pure water (control condition) for 2 or 24 h in the presence of 0.4% ethanol (EtOH). After LPS treatment the medium was removed, cells were washed three times with PBS, scraped off with 800 μl PBS, lipids were extracted and radiolabeled phosphatidylethanol ([^{3}H]-PEth), an unequivocal PLD activity marker, was separated as previously described in our lab (Mateos et al., 2010; Salvador and Giusto, 1998).

2.9. Western blot analysis

For Western blot assays (WB) cells were washed three times with PBS and scraped off with 80 μl ice-cold RIPA lyses buffer (10 mM Tris–HCl (pH 7.4), 15 mM NaCl, 1% Triton X-100, 5 mM NaF, 1 mM Na_2VO_4 and the complete protease inhibitor cocktail). Protein content of cellular lysates was determined by Bradford method (Bradford, 1976) (Bio-Rad Life Science group, #500-0006). Samples were subsequently denatured with Laemmli sample buffer at 100°C for 5 min (Laemmli, 1970). Equivalent amounts of proteins (30 μg) were separated by sodium dodecyl sulfatepolyacrylamide gel electrophoresis (SDS-PAGE) on 10% polyacrylamide gels and subsequently transferred to polyvinylidene fluoride (PVDF) membranes (Millipore, Bedford, MA, USA) which were blocked with 10% BSA in TTBS buffer [20 mM Tris–HCl (pH 7.4), 100 mM NaCl and 0.1% (w/v) Tween 20] at room temperature for 2 h. Membranes were subsequently incubated with primary antibodies for 2 h at room temperature, washed three times with TTBS and then exposed to the appropriate HRP-conjugated secondary antibody (anti-rabbit or anti-mouse) for 2 h at room temperature. Immunoreactive bands were detected by enhanced chemiluminescence (ECL prime, Amersham Biosciences) using standard X-ray film (Kodak X-Omat AR).

2.10. Plasmids and DNA transfection

Plasmids encoding the EGFP-tagged versions of wild-type PLDs (pEGFP-C1-hPLD1b and pEGFP-C1-mPLD2) and the inactive mutant of PLD1 (pEGFP-C1-hPLD1b^{K898R}) were kindly provided by Dr. Xosé Bustelo (Centro de Investigación del Cáncer, University of Salamanca, Spain). In the inactive mutant of PLD1 the K898, found in the second HKD motif, was substituted by an arginine. This mutation resulted in a complete loss of enzymatic activity without affecting the folding of the protein, the subcellular localization under basal conditions or the interaction with cofactors such as RhoA and ARF (Sung et al., 1997). Cells grown onto coverslips (30–50% confluence) were transiently transfected using Lipofectamine 2000 (LifeTechnologies™) according to the protocol provided by the manufacturer. LPS stimulation was performed 24 h after transfection.

2.11. Wide-field fluorescence microscopy

Living unfixed cells were imaged with a Nikon Eclipse E-600 microscope 24 h after transfection. Imaging was done with an SBIG model ST-7 digital charge-coupled device camera (765 × 510 pixels, 9.0 × 9.0 μm pixel size; Santa Barbara, CA, USA). For all experiments a 40× (1.0 N.A.) objective was used.

2.12. Confocal microscopy

After transfection and LPS treatment (10 μg/ml for 24 h), cells were fixed and permeabilized and nuclei were stained using TO-PRO®-3 (Life Technologies). Then cells were imaged using a TCS-SP2 confocal microscope (Leica Mikrosysteme Vertrieb GmbH, Wetzlar, Germany) equipped with an acoustooptical beam splitter. For all experiments a 63× (1.2 N.A.) objective was used.

2.13. Statistical analysis

Statistical analysis was performed using ANOVA followed by Bonferroni's test to compare means. *p*-Values lower than 0.05 were considered statistically significant. Data represent the mean value ± SD of three independent experiments. The WBs shown are a representative image of samples from three independent experiments.

3. Results

3.1. Characterization of LPS effect on ARPE-19 cells

In order to establish and characterize a model of inflammation in RPE, ARPE-19 cells were treated with LPS (0, 5, 10 and 100 μg/ml) for 24, 48 and 72 h. WB assays showed that ARPE-19 cells express the primary LPS receptor, CD14, and its membrane-linked co-receptor, toll-like receptor 4 (TLR4). Furthermore, after 24 h treatment with different LPS concentrations the expression of these proteins was observed not to be significantly affected (Fig. 1A). Fig. 1B shows that LPS (10 μg/ml) treatment for 24 and 48 h increased NO production by RPE cells with respect to the control condition (100 and 180%, respectively). Mitochondrial function was analyzed using MTT reduction assay. Fig. 1C shows that a 24 h treatment with LPS (5, 10 and 100 μg/ml) did not affect ARPE-19 metabolic state. However, after a 48 and 72 h treatment with LPS 5, 10 and 100 μg/ml, MTT reduction was reduced by 10, 15 and 20% with respect to the control condition, respectively (Fig. 1C). On the contrary, no LDH leakage to the culture medium was detected after LPS (5, 10 and 100 μg/ml) treatment for 24, 48 and 72 h, indicating that plasma membrane integrity was not affected under our experimental conditions.

3.2. COX-2 induction and PGs production in ARPE-19 cells exposed to LPS

It is well known that COX-2 can be induced in RPE cells by several stimuli, such as LPS and proinflammatory cytokines (Fang et al., 2007; Chin et al., 2001). After characterizing the effect of LPS on ARPE-19 cells, we further investigated the state of COX-2 in our experimental setup. Fig. 2A shows that in ARPE-19 cells LPS (10 μg/ml) treatment for 24 h induced a 100% increase in the expression of COX-2 with respect to the control condition. As expected, the expression of the constitutive isoform COX-1 was

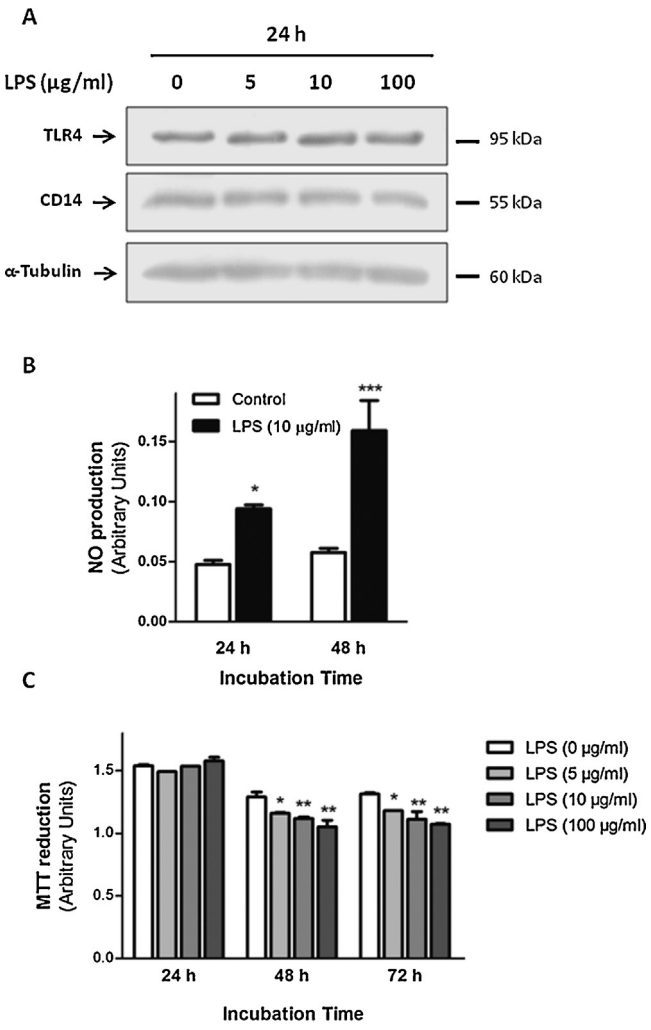

Fig. 1. Characterization of LPS effect on ARPE-19 cells. (A) ARPE-19 cells were incubated with LPS (5, 10, 100 μg/ml) or ultra pure water (control condition) for 24 h. TLR4 and CD14 expression in ARPE-19 cells was analyzed by WB assays as detailed in Materials and Methods. Numbers to the right indicate molecular weights designated by standard markers. One representative image of three independent WB is shown. (B) NO production by ARPE-19 cells was analyzed in cells treated with LPS (10 μg/ml) or under control conditions for 24 and 48 h as detailed in Materials and Methods. Data represent the mean value ± SD of three independent experiments. Results are expressed as arbitrary units. (C) Mitochondrial function was evaluated using the MTT reduction assay in ARPE-19 cells treated with LPS (5, 10, 100 μg/ml) or ultra pure water (control condition) for 24, 48 and 72 h. Data represent the mean value ± SD of four independent experiments. Results are expressed as arbitrary units. Asterisks indicate significant differences with respect to each control condition (* $p < 0.05$; ** $p < 0.01$).

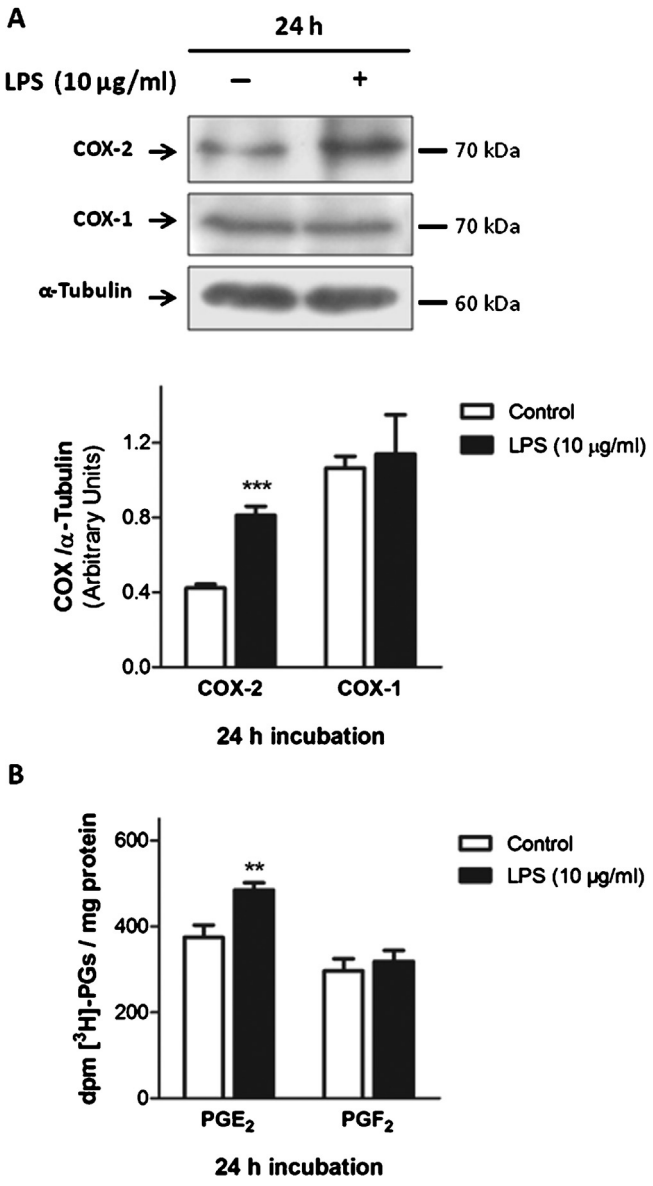

Fig. 2. COX-2 induction and PGs production in ARPE-19 cells exposed to LPS. (A) ARPE-19 cells treated with LPS (10 μg/ml) or under control conditions for 24 h. WB assays to detect COX-2 and COX-1 were performed as described in Materials and Methods. Numbers to the right indicate molecular weights. One representative image of four independent WB is shown. The bar graph shows the densitometry values of each COX/α-Tubulin. (B) ARPE-19 cells were incubated for 24 h with [^{3}H]-AA and [^{3}H]-PGs produced and secreted to the media were isolated and quantified as described in Materials and Methods. Data represent the mean value ± SD of three independent experiments. Results are expressed as dpm [^{3}H]-PGs/mg protein. Asterisks indicate significant differences with respect to the control condition (** $p < 0.01$, *** $p < 0.001$).

not affected by LPS treatment (Fig. 2A). To analyze COX activity PGs generation was measured in ARPE-19 cells treated for 24 h with LPS (10 μg/ml) or under control conditions. To this end, cells were prelabeled with [^{3}H]-AA and [^{3}H]-PGE_2 and [^{3}H]-PGF_2 secreted to the medium were measured. [^{3}H]-PGE_2 production increased by 30% in RPE cells treated with LPS (10 μg/ml) for 24 h with respect to untreated cells. PGF_2 production was not affected by LPS treatment (Fig. 2B).

3.3. PLDs expression, subcellular localization and activation in ARPE-19 cells exposed to LPS

We next investigate if PLD pathway was able to modulate the inflammatory response induced by LPS in RPE cells. There are, in fact, no previous reports on either the presence or function of PLD isoforms in RPE cells. WB assays showed that PLD1 and PLD2 are expressed in ARPE-19 cells (Fig. 3A). We subsequently investigated the subcellular localization of PLD1 and PLD2. ARPE-19 cells were transiently transfected with plasmids encoding EGFP-tagged PLD1 and PLD2 and living and unfixed cells were imaged using wide-field microscopy. Fig. 3B shows that EGFP-PLD1 was present in punctuate perinuclear and cytoplasmic structures while EGFP-PLD2 was present in the plasma membrane (Fig. 3B).

It is well known that in the presence of primary alcohols, only classical PLDs are able to catalyze a transphosphatidylation reaction yielding phosphatidylalcohols instead of PA. Thus, phosphatidylalcohol generation blocks LPPs action and prevents

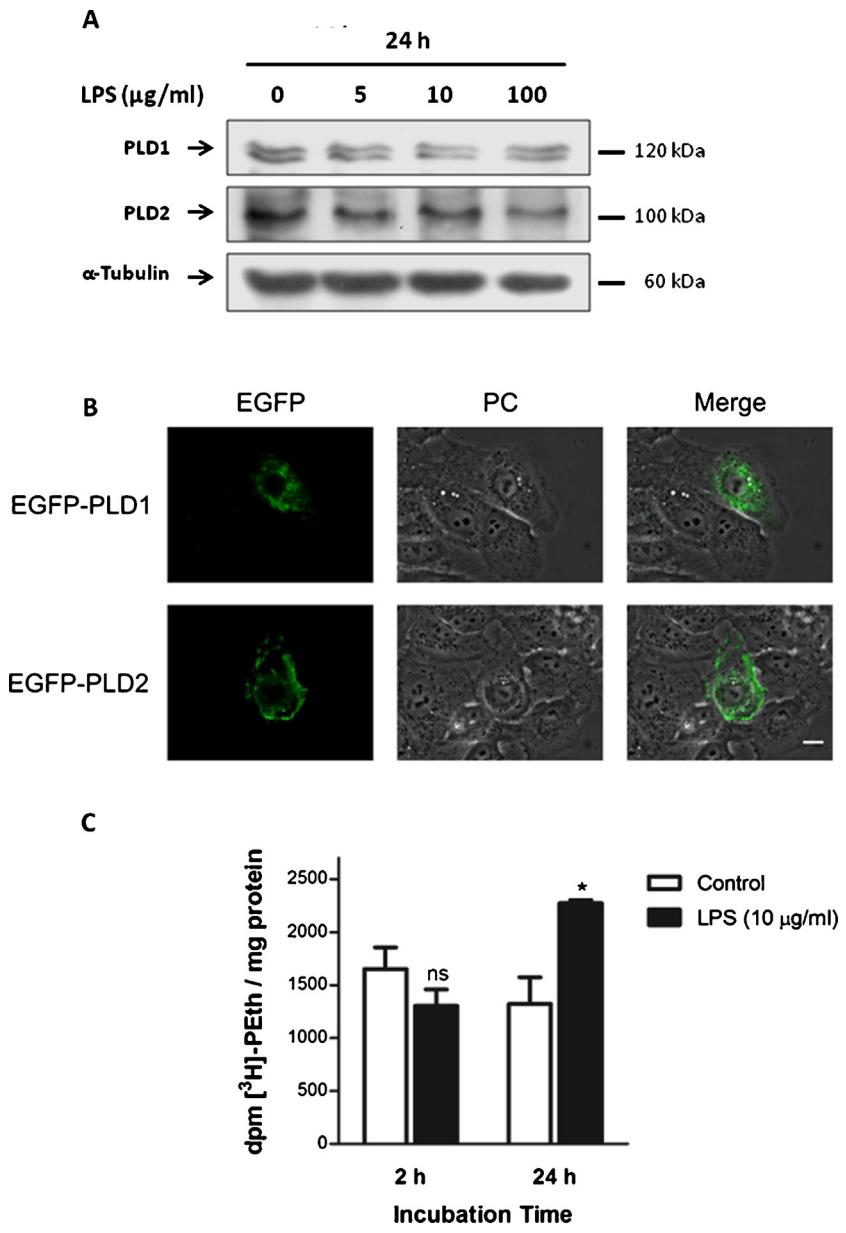

Fig. 3. PLDs expression, subcellular localization and activation in ARPE-19 cells exposed to LPS. (A) ARPE-19 cells were treated with LPS (5, 10, 100 μg/ml) or ultra pure water (control condition) for 24 h and the expression of PLD1 and PLD2 was analyzed by WB as described in Materials and Methods. One representative image of four independent WB is shown. Numbers to the right indicate molecular weights. (B) PLD1 and PLD2 subcellular localization in ARPE-19 cells. ARPE-19 cells were grown onto coverslips and transfected with vectors encoding the EGFP-tagged versions of PLD1 and PLD2 (EGFP-PLD1 and EGFP-PLD2). Cells were analyzed 24 h post transfection by wide-field fluorescence microscopy. Representative images from three different experiments are shown. PC—phase contrast, scale bar = 10 μm. (C) PLD activity was measured as [^{3}H]-PEth formation in cells preincubated with [^{3}H]-OA and treated with LPS (10 μg/ml) or under control conditions for 2 or 24 h in the presence of 0.4% EtOH. Data represent the mean value ± SD of three independent experiments. Results are expressed as dpm [^{3}H]-PEth/mg protein. Asterisks indicate significant differences with respect to the control condition (* $p < 0.05$).

DAG formation from occurring via PLD/LPPs pathway (Mateos et al., 2010, 2008). In order to study the effect of LPS treatment on PLD activity, [^{3}H]-OA prelabeled cells were treated with LPS (10 μg/ml) for 2 and 24 h in the presence of 0.4% ethanol (EtOH) and phosphatidylethanol ([^{3}H]-PEth) generation was measured. However, only LPS treatment for 24 h increased [^{3}H]-PEth generation by 90% with respect to untreated cells (Fig. 3C). These results demonstrate that in ARPE-19 cells not only PLD1 and PLD2 are expressed but also that PLDs are activated by LPS treatment.

To corroborate and to study the effect of LPS on PLD1 and PLD2 subcellular localization, ARPE-19 cells were transfected with EGFP-tagged PLDs, fixed and permeabilized. Nuclei were stained with TO-PRO-3 and confocal microscopy was done. Confocal images confirmed EGFP-PLD1 punctate perinuclear localization under control conditions as well as EGFP-PLD2 plasma membrane localization (Fig. 4A and B first set of images). When EGFP-PLD1 expressing cells were treated with LPS (10 μg/ml) for 24 h, only 17 ± 3.6% of the cells showed EGFP-PLD1perinuclear localization, 63 ± 6.66% of the cells evidenced a diffuse localization of PLD1 (Fig. 4A, second set of images) and 20 ± 8.96% of the cells evidenced a plasma membrane localization (Fig. 4A, third set of images). In contrast, LPS treatment did not modify EGFP-PLD2 localization, thus indicating that this isoform remains exclusively located in plasma membrane domains (Fig. 4B, second set of images). Same results were obtained in living unfixed cells (Data not shown).

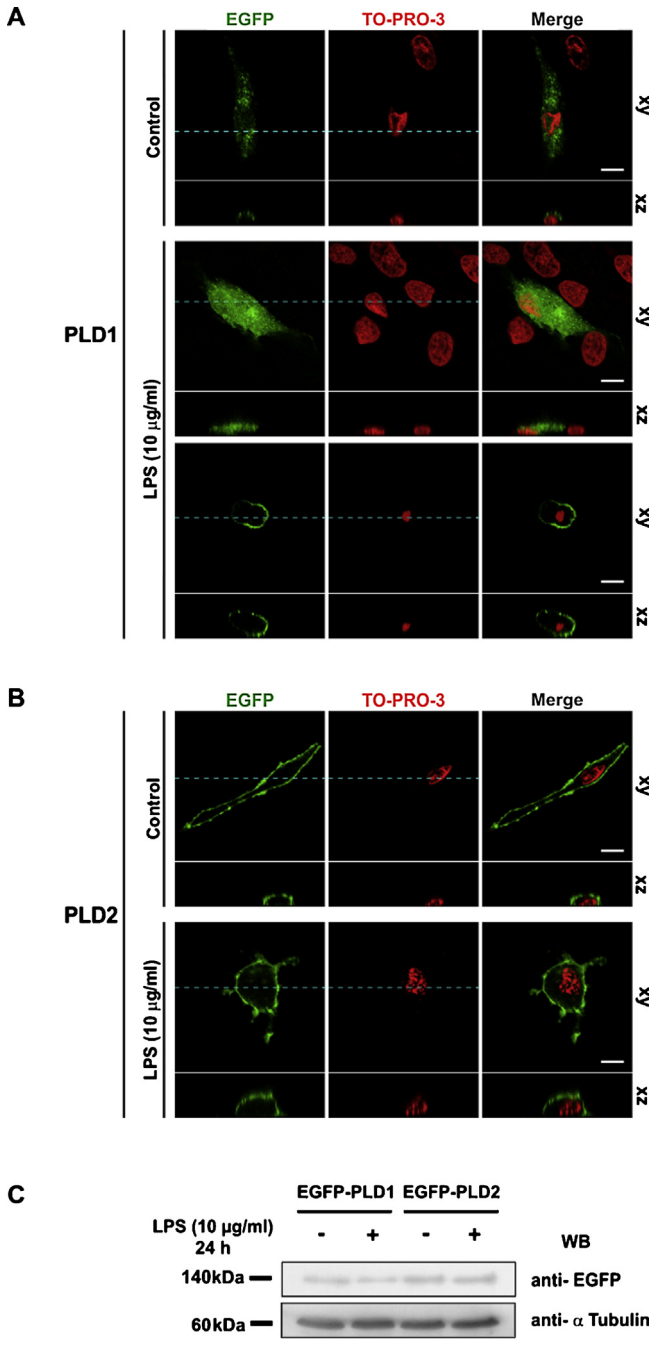

Fig. 4. PLD1 and PLD2 subcellular localization in ARPE-19 cells exposed to LPS. ARPE-19 cells were grown onto coverslips and transfected with vectors encoding the EGFP-tagged versions of wild type PLD1 (EGFP-PLD1; (A) and PLD2 (EGFP-PLD2; (B). 24 h post transfection cells were treated under control conditions or with 10 μg/ml LPS for 24 h. Then, cells were fixed, permeabilized and stained with TO-PRO-3 to visualize the nuclear structure. EGFP and TO-PRO-3 were imaged with a confocal microscopy, where *xy* and vertical *xz* slices, from *xy* regions marked with dashed lines, were acquired. Representative images from three different experiments are shown. Scale bar = 10 μm. (C) WB assays were performed using anti-EGFP antibody to check the molecular weight of the EGFP-PLDs. Numbers to the left indicate molecular weights.

In order to study whether these LPS-induced changes in PLD1 localization are dependent on PLD1 activation, ARPE-19 cells were transfected with a plasmid encoding the EGFP-tagged inactive mutant of PLD1 (EGFP-PLD1^{K898R}) and then treated with 10 μg/ml LPS for 24 h. As observed in wild type PLD1 expressing cells, EGFP-PLD1^{K898R} was also found to evidence punctuate perinuclear and cytoplasmic localization under control conditions (Fig. 5A, first set

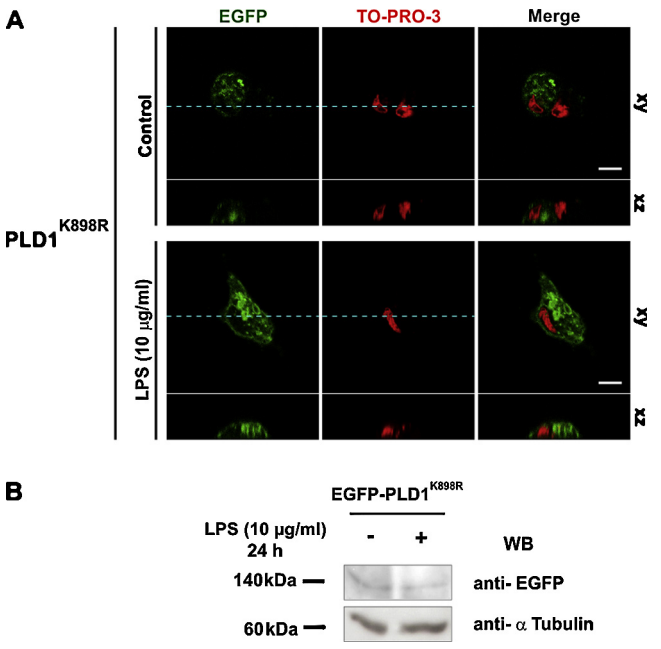

Fig. 5. PLD1 inactive mutant subcellular localization in ARPE-19 cells exposed to LPS. (A) ARPE-19 cells were grown onto coverslips and transfected with vectors encoding the EGFP-tagged version of the inactive mutant of PLD1 (EGFP-PLD1^{K898R}). 24 h post transfection cells were treated under control conditions or with 10 μg/ml LPS for 24 h. Then, cells were fixed, permeabilized and stained with TO-PRO-3 to visualize the nuclear structure. EGFP and TO-PRO-3 were imaged with a confocal microscopy, where *xy* and vertical *xz* slices, from *xy* regions marked with dashed lines, were acquired. Representative images from three different experiments are shown. Scale bar = 10 μm. (B) WB assays were performed using anti-EGFP antibody to check the molecular weight of EGFP-PLD1^{K898R}. Numbers to the left indicate molecular weights.

of images). However, LPS treatment did not significant modify the localization of the inactive mutant of PLD1 (Fig. 5A, second set of images). The *xy* and vertical *xz* analysis of the slices corroborated the subcellular localization of EGFP-PLDs and same results were obtained in living unfixed cells (Data not shown). WB assays using anti-EGFP antibody showed the presence of an immunoreactive band corresponding to the molecular weight of PLDs plus the molecular weight of EGFP (≈140 kDa) (Figs. 4C and 5B).

3.4. Role of PLDs pathway in ERK1/2 activation in ARPE-19 cells exposed to LPS

We next investigated the state of ERK1/2 activation in ARPE-19 cells challenged with LPS. WB assays showed that in ARPE-19 cells, LPS (5, 10 and 100 μg/ml) treatment for 24 h increased ERK1/2 phosphorylation (activation) by 150, 225 and 75%, respectively (Fig. 6A).

Then we studied the role of PLD in ERK1/2 activation. On account of the fact that PEth formation did not distinguish between PLD1 and PLD2 activity because both isoforms have the ability to catalyze the transphosphatidylation reaction, cells were preincubated with selective PLD inhibitors for 1 h before LPS treatment: 0.15 μM EVJ (PLD1 inhibitor) and 0.5 μM APV (PLD2 inhibitor) in order to study the role of each isoform in ERK1/2 activation. The effectiveness of these compounds for selectively inhibiting PLDs was previously tested in our lab and also by other authors (Cheol et al., 2013; Liu et al., 2013; Mateos et al., 2012; Scott et al., 2009). Furthermore, in order to inhibit DAG generation from phosphatidylinositol (4, 5) bisphosphate phospholipase C (PIP_2-PLC) pathway we used U73122 (10 μM) and U0126 (10 μM) to inhibit MEK, which is the immediate upstream regulator of ERK1/2 (Mateos et al., 2012).

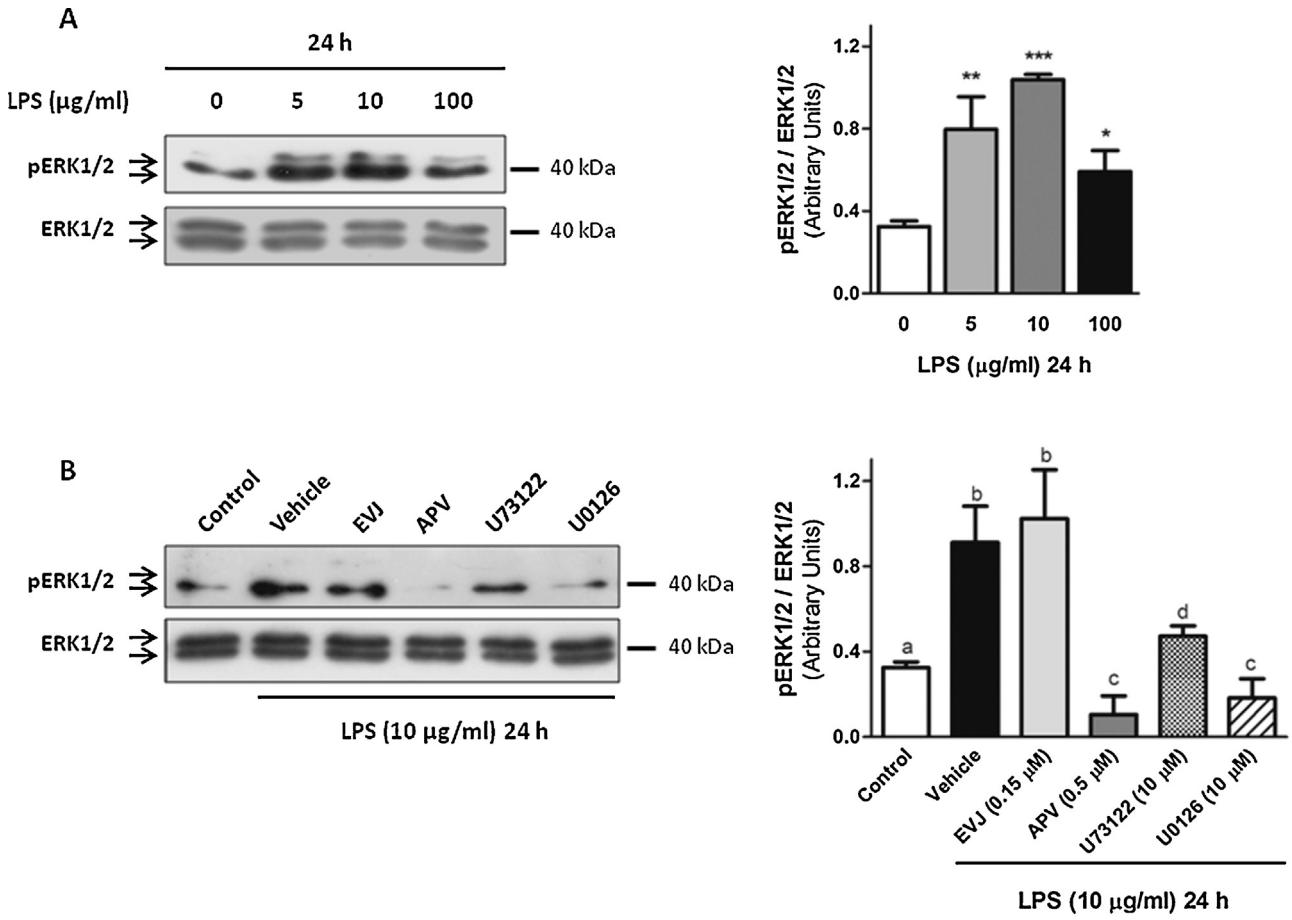

Fig. 6. Role of PLD pathways in ERK1/2 activation. (A) ERK1/2 activation in ARPE-19 cells exposed to LPS. ARPE-19 cells were treated with LPS (0, 5, 10, 100 μg/ml) for 24 h. ERK1/2 activation was evaluated by WB assays using anti-phosphoERK1/2 (pERK1/2) antibody. (B) ARPE-19 cells were preincubated with 0.025% DMSO (Control and Vehicle conditions), 0.15 μM EVJ, 0.5 μM APV, 10 μM U73122 or 10 μM U0126 for 1 h before LPS treatment. Cells were treated with 10 μg/ml LPS or ultra pure water (Control condition) for 24 h and ERK1/2 activation was evaluated by WB assays using anti-phosphoERK1/2 (pERK1/2) antibody. The bar graph shows the densitometry values of pERK1/2/ERK1/2 expressed as arbitrary units. Asterisks indicate significant differences with respect to the control condition (* $p < 0.05$; ** $p < 0.01$ *** $p < 0.001$). Conditions designated with different letters ((a)–(d)) present significant differences ($p < 0.05$) between them. One representative image of three independent WB is shown. Numbers to the right indicate molecular weights.

In ARPE-19 cells, ERK1/2 activation after 24 h treatment with LPS was completely abolished by the preincubation with APV, PLD2 inhibitor, but it was not affected by the inhibition of PLD1 with EVJ (Fig. 6B). PIP_2-PLC inhibition only partially reduced ERK1/2 activation and, as expected, the inhibition of MEK with U0126 was found to abolish ERK1/2 phosphorylation (Fig. 6B).

3.5. Role of PLD pathways in COX-2 activation and RPE mitochondrial function

We next investigated the role of PLD isoforms in COX-2 regulation. For this end, APV and EVJ were used as PLD inhibitors. COX-2 induction by LPS was, in turn, dependent on both PLD isoforms and the MEK/ERK1/2 pathway but was not significantly affected by PIP_2-PLC inhibition while COX-1 expression was observed to remain unaffected under all conditions (Fig. 7A). As it was expected, the preincubation of the cells with the inhibitors that reduced COX-2 induction (APV, EVJ and U0126) also abolished [^{3}H]-PGE_2 production induced by 24 h treatment with LPS (Fig. 7B). In order to study the role of PLD1, PLD2, ERK1/2 and COX-2 in the reduced RPE mitochondrial metabolic state induced by LPS, ARPE-19 cells were preincubated with the aforementioned inhibitors before LPS (10 μg/ml) treatment for 48 h and mitochondrial function was analyzed by MTT reduction assay. Cells were also preincubated with EtOH (0.4%) to block PA and DAG generation from both PLDs and with Celecoxib (10 μM) to inhibit COX-2 activity. None of the inhibitors affected MTT reduction under control conditions (Data not shown). The loss in mitochondrial function induced by LPS was prevented by EtOH and by the inhibition of PLD2, the MEK/ERK1/2 pathway and COX-2 (Fig. 7C). However, neither PLD1 nor PIP_2-PLC inhibition was observed to counteract the effect of LPS on the metabolic state of the cells (Fig. 7C).

4. Discussion

The inflammatory process is part of the pathophysiology of several diseases of the retina, including AMD, RP, uveitis and diabetic retinopathy (DR) (Perez et al., 2013; Tarr et al., 2013; Viringipurampeer et al., 2013; Whitcup et al., 2013a). During these pathological conditions the RPE plays key immunological roles, exerting macrophage and microglia-like functions (Whitcup et al., 2013b; Leung et al., 2009). It was previously demonstrated that RPE cells isolated from human healthy donors express the CD14/TLR4 LPS-recognizing complex (Elner et al., 2005). Furthermore, LPS can directly stimulate RPE cells in situations of acute ocular inflammation, such as bacterial endophthalmitis and uveitis (Pollreisz et al., 2012; Leung et al., 2009) and this bacterial endotoxin can also reach RPE cells in postsurgical and posttraumatic infections (Pollreisz et al., 2012). After 24 h with LPS ARPE-19 cells showed increased levels of NO production and a reduced mitochondrial

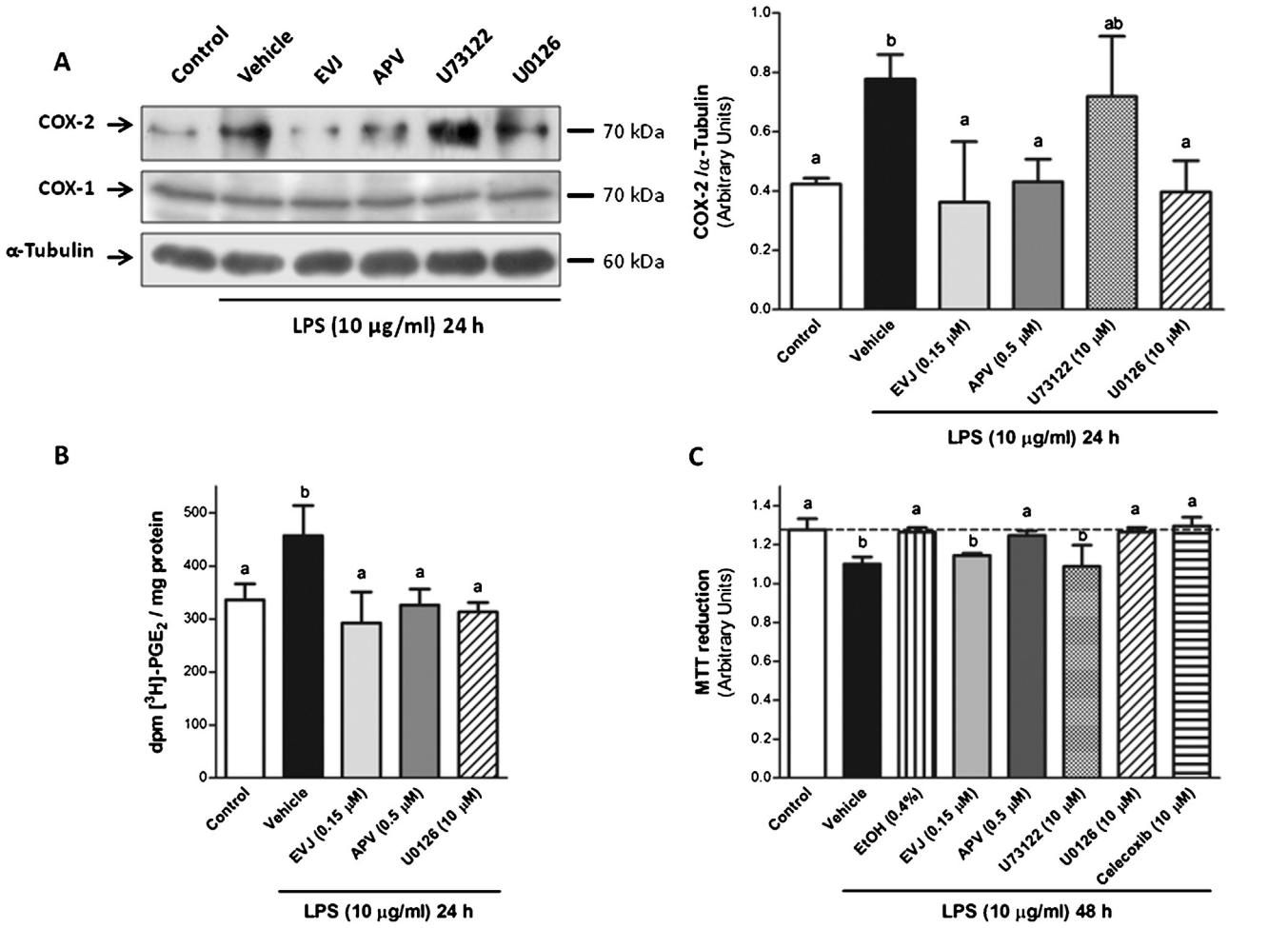

Fig. 7. Role of PLD pathways in COX-2 induction, PGE_2 production and mitochondrial function. (A) COX-1 and COX-2 induction in ARPE-19 cells was determined by WB in cells previously treated with 0.025% DMSO (Control and Vehicle conditions), or with 0.15 μM EVJ, 0.5 μM APV, 10 μM U73122, 10 μM U0126. Numbers to the right indicate molecular weights and the bar graph shows the densitometry values of COX-2/α-Tubulin expressed as arbitrary units. Conditions designated with different letters ((a)–(b)) present significant differences ($p < 0.05$) between them. One representative image of three independent WB is shown. (B) [^{3}H]-PGE_2 production was measured as described in Materials and Methods in cells preincubated for 1 h with 0.025% DMSO (Control and Vehicle conditions), 0.15 μM EVJ, 0.5 μM APV or with 10 μM U0126 before 10 μg/ml LPS treatment for 24 h. Data represent the mean value ± SD of three independent experiments. Results are expressed as dpm [^{3}H]-PGE_2/mg protein. Conditions designated with different letters ((a)–(b)) present significant differences ($p < 0.05$) between them. (C) ARPE-19 cells were preincubated with 0.4% EtOH, 0.15 μM EVJ, 0.5 μM APV, 10 μM U73122, 10 μM U0126 or 10 μM Celecoxib for 1 h before LPS treatment. Cells were treated with 10 μg/ml LPS or ultra pure water (Control condition) for 48 h and mitochondrial function was evaluated using MTT reduction assay. Results are expressed as arbitrary units. Conditions designated with different letters ((a)–(b)) present significant differences ($p < 0.05$) between them.

function (Fig. 1B and C). In addition, the increased levels of COX-2 observed in ARPE-19 cells exposed to LPS for 24 h, together with the enhanced PGE_2 production, reinforce the validity of this inflammation model (Fig. 2). This increased COX-2 expression and the production of PGs induced by LPS in ARPE-19 cells is in accordance with previous reports on human RPE cells from healthy donor eyes (Chin et al., 2001).

After 48 h of treatment with 10 μg/ml LPS MTT reduction was reduced by 15% with respect to the control condition (Fig. 1C). Although this reduction is significant, it does not represent a massive loss of mitochondrial viability under our experimental conditions, thus indicating that RPE cells are extremely resistant cells capable of dealing with different threats (such as toxins, UV light and reactive oxygen species) to protect the neural retina (Faghiri and Bazan, 2010). Nevertheless, taking into account that RPE is a monolayer of cells that forms part of the blood-retina barrier, and that in the human fovea each RPE cell is in contact with an average of 23 PRs (Strauss, 2005), minor changes in RPE cell viability could lead to an important PR damage and, in consequence, to loss of vision in vivo.

Previous reports have shown that the PLD pathway plays important roles in macrophage functions, such as chemotaxis, phagocytosis, iNOS expression and NO production (Ali et al., 2013; Kantonen et al., 2011; Knapek et al., 2010; Park et al., 2010; Zhang et al., 2001). However, findings from our study demonstrate for the very first time that PLD1 and PLD2 exert key functions during the inflammatory process in RPE cells through ERK1/2 activation and COX-2 expression. Further experiments would be needed to elucidate the role of the PLD pathway in iNOS expression and NO production during RPE inflammatory response.

Both the generation of PEth (a specific PLD activity marker) and WB assays demonstrate for the first time that ARPE-19 cells express PLD1 as well as PLD2 isoforms and that LPS increases PLD activity after 24 h of treatment (Fig. 3A and C). Furthermore, even though PEth generation does not distinguish between PLD1 and PLD2 activity, the differential effects of selective PLD inhibitors (EVJ and APV) on ERK1/2 activation (Fig. 6B), COX-2 induction and PGE_2 production and MTT reduction (Fig. 7) demonstrate that both PLD isoforms are activated by LPS.

EGFP-PLDs expressing ARPE-19 cells showed the typical localization previously reported for PLD1 and PLD2, PLD1 was predominantly localized under steady-state conditions in punctuate perinuclear and cytoplasmic structures whereas PLD2 was found at the plasma membrane (Figs. 3B and 4). Our results showed that after 24 h treatment with LPS PLD1 is able to translocate to the plasma membrane (Fig. 4A) and this translocation is dependent on PLD1 activity, since the inactive mutant ($PLD1^{K898R}$) was unable to translocate after LPS stimulation (Fig. 5A). These results are in agreement with previous reports that showed that upon stimulation PLD1 translocates from perinuclear structures to the plasma membrane in RBL-2H3 and COS-7 cells (Du et al., 2003; Brown et al., 1998). Moreover, the translocation of the inactive mutant $PLD1^{K898R}$ was substantially decreased with respect to the wild type PLD1 in stimulated COS-7 cells, indicating that the translocation is facilitated when PLD1 is capable of being activated (Du et al., 2003). Our results together with these previous reports suggest that the localization of the PLD1 is not static and that translocation may be crucial for triggering signaling pathways at the plasma membrane level in LPS-stimulated RPE cells.

ERK1/2 activation induced by LPS has been observed in several types of macrophages and it has been proposed as a modulator of important immunological functions. Inhibition of ERK1/2 blocks macrophage activation and TNF-α and IL-1β production (Valledor et al., 2000). ERK1/2 and S6K1 activation was found to mediate iNOS expression and NO production in a PLD2-dependent manner (Park et al., 2010). Our results constitute the first evidence of PLD2 dependent LPS-induced ERK1/2 activation in RPE cells (Fig. 6B, see graphical abstract).

COX-2 induction and PGE_2 production in LPS stimulated ARPE-19 cells was observed to be dependent on PLD1 and PLD2 activity and the MEK/ERK1/2 pathway (Fig. 7A and B). Taking into account that LPS-induced ERK1/2 activation was abolished by PLD2 inhibition but was not affected by preincubation the PLD1 inhibitor, our results suggest that PLD2 mediates COX-2 induction through the activation of the MEK/ERK1/2 pathway while PLD1 mediates COX-2 expression through an ERK-independent mechanism. Our results agree with a previous research according to which COX-2 induction in ARPE-19 cells either treated with linoleic acid or exposed to UV light was also dependent on ERK1/2 activation (Chan et al., 2008; Fang et al., 2007). PLD1 and PLD2 have been also found to be involved in COX-2 induction and PGE_2 production in several cell types (Ahn et al., 2007; Kim et al., 2004; Grab et al., 2004). Nevertheless, our work constitutes the first report of PLD dependent COX-2 expression in RPE.

The inhibition of PLD2, ERK1/2 and COX-2 restored MTT reduction to control levels (Fig. 7C). These data demonstrate that the PLD2-ERK1/2-COX-2-PGE_2 pathway could lead to RPE cell damage, possibly through PGE_2 paracrine or autocrine effects. However, our results agree with previous findings that demonstrate that ERK1/2 activation triggers RPE cell death in the chronic nature of macular degeneration progression (Dridi et al., 2012). On the other hand, PLD1 and PIP_2-PLC inhibitors were observed not to be able to prevent the loss in mitochondrial function as a result of LPS treatment. It is thus interesting to note that inhibition of PLD1 did not prevent LPS-induced cell damage while it did inhibit COX-2 expression and PGE_2 production. This could suggest that PLD1 plays a dual role under inflammatory conditions in the RPE: by promoting cell damage through an ERK1/2-independent COX-2 induction and by modulating cellular protective mechanisms.

5. Conclusion

Our results demonstrate that after sustained stimulation of RPE cells with LPS, the subsequent activation of PLD2, ERK1/2 and the induction in the expression of COX-2 mediates cell damage. Based on our findings, PLD2 and ERK1/2 could be considered as potential therapeutic targets for ocular inflammatory diseases treatments.

Funding

This work was supported by grants from the Universidad Nacional del Sur (PGI 24B169), the Consejo Nacional de Investigaciones Científicas y Técnicas (PIP 11220090100687-CONICET) and the Agencia Nacional de Promoción Científica y Tecnológica (ANPCYT PICT 2010-0936). MVM, GAS and NMG are research members of CONICET, CBK is a doctoral fellow from CONICET.

Acknowledgements

Authors want to thank Dr. Xosé Bustelo from the "*Centro de Investigación del Cáncer*" (CIC), University of Salamanca, Spain, for kindly providing plasmids encoding the EGFP-tagged versions of PLDs and Lic. Edgardo Buzzi for his technical assistance in cell culture and confocal microscopy. Authors are also grateful to Translator Viviana Soler for her technical assistance in controlling the use of the English language.

References

Ahn BH, Park MH, Lee YH, Kwon TK. Min dS. Up-regulation of cyclooxygenase-2 by cobalt chloride-induced hypoxia is mediated by phospholipase D isozymes in human astroglioma cells. Biochim Biophys Acta 2007;1773:1721–31.

Ali WH, Chen Q, Delgiorno KE, Su W, Hall JC, Hongu T, et al. Deficiencies of the lipid-signaling enzymes phospholipase D1 and D2 alter cytoskeletal organization, macrophage phagocytosis, and cytokine-stimulated neutrophil recruitment. PLoS One 2013;8:e55325.

Bradford MM. A rapid and sensitive method for the quantitation of microgram quantities of protein utilizing the principle of protein-dye binding. Anal Biochem 1976;72:248–54.

Brown FD, Thompson N, Saqib KM, Clark JM, Powner D, Thompson NT, et al. Phospholipase D1 localises to secretory granules and lysosomes and is plasma-membrane translocated on cellular stimulation. Curr Biol 1998;8:835–8.

Chan CM, Huang JH, Lin HH, Chiang HS, Chen BH, Hong JY, et al. Protective effects of (−)-epigallocatechin gallate on UVA-induced damage in ARPE19 cells. Mol Vision 2008;14:2528–34.

Cheol SJ, Woo KD, Mo YK, Choi KY, Gen ST, Min dS. Phospholipase D inhibitor enhances radiosensitivity of breast cancer cells. Exp Mol Med 2013;45:e38.

Chin MS, Nagineni CN, Hooper LC, Detrick B, Hooks JJ. Cyclooxygenase-2 gene expression and regulation in human retinal pigment epithelial cells. Invest Ophthalmol Vis Sci 2001;42:2338–46.

Cutini PH, Campelo AE, Agriello E, Sandoval MJ, Rauschemberger MB, Massheimer VL. The role of sex steroids on cellular events involved in vascular disease. J Steroid Biochem Mol Biol 2012;132:322–30.

Dridi S, Hirano Y, Tarallo V, Kim Y, Fowler BJ, Ambati BK, et al. ERK1/2 activation is a therapeutic target in age-related macular degeneration. Proc Natl Acad Sci USA 2012;109:13781–6.

Du G, Altshuller YM, Vitale N, Huang P, Chasserot-Golaz S, Morris AJ, et al. Regulation of phospholipase D1 subcellular cycling through coordination of multiple membrane association motifs. J Cell Biol 2003;162:305–15.

Dixon DA, Blanco FF, Bruno A, Patrignani P. Mechanistic aspects of COX-2 expression in colorectal neoplasia. Recent Results Cancer Res 2013;191:7–37.

Elner SG, Petty HR, Elner VM, Yoshida A, Bian ZM, Yang D, et al. TLR4 mediates human retinal pigment epithelial endotoxin binding and cytokine expression. Trans Am Ophthalmol Soc 2005;103:126–35.

Faghiri Z, Bazan NG. PI3K/Akt and mTOR/p70S6K pathways mediate neuroprotectin D1-induced retinal pigment epithelial cell survival during oxidative stress-induced apoptosis. Exp Eye Res 2010;90:718–25.

Fang IM, Yang CH, Yang CM, Chen MS. Linoleic acid-induced expression of inducible nitric oxide synthase and cyclooxygenase II via p42/44 mitogen-activated protein kinase and nuclear factor-kappaB pathway in retinal pigment epithelial cells. Exp Eye Res 2007;85:667–77.

Grab LT, Kearns MW, Morris AJ, Daniel LW. Differential role for phospholipase D1 and phospholipase D2 in 12-*O*-tetradecanoyl-13-phorbol acetate-stimulated MAPK activation, Cox-2 and IL-8 expression. Biochim Biophys Acta 2004;1636:29–39.

He D, Natarajan V, Stern R, Gorshkova IA, Solway J, Spannhake EW, et al. Lysophosphatidic acid-induced transactivation of epidermal growth factor receptor regulates cyclo-oxygenase-2 expression and prostaglandin E(2) release via C/EBPbeta in human bronchial epithelial cells. Biochem J 2008;412:153–62.

Ishida K, Panjwani N, Cao Z, Streilein JW. Participation of pigment epithelium in ocular immune privilege, 3. Epithelia cultured from iris, ciliary body, and retina suppress T-cell activation by partially non-overlapping mechanisms. Ocul Immunol Inflamm 2003;11:91–105.

Jenkins GM, Frohman MA. Phospholipase D: a lipid centric review. Cell Mol Life Sci 2005;62:2305–16.
Kantonen S, Hatton N, Mahankali M, Henkels KM, Park H, Cox D, et al. A novel phospholipase D2-Grb2-WASp heterotrimer regulates leukocyte phagocytosis in a two-step mechanism. Mol Cell Biol 2011;31:4524–37.
Kim SY, Ahn BH, Min KJ, Lee YH, Joe EH, Min DS. Phospholipase D isozymes mediate epigallocatechin gallate-induced cyclooxygenase-2 expression in astrocyte cells. J Biol Chem 2004;279:38125–33.
Knapek K, Frondorf K, Post J, Short S, Cox D, Gomez-Cambronero J. The molecular basis of phospholipase D2-induced chemotaxis: elucidation of differential pathways in macrophages and fibroblasts. Mol Cell Biol 2010;30:4492–506.
Laemmli UK. Cleavage of structural proteins during the assembly of the head of bacteriophage T4. Nature 1970;227:680–5.
Lamb TD, Collin SP, Pugh EN Jr. Evolution of the vertebrate eye: opsins, photoreceptors, retina and eye cup. Nat Rev Neurosci 2007;8:960–76.
Leung KW, Barnstable CJ, Tombran-Tink J. Bacterial endotoxin activates retinal pigment epithelial cells and induces their degeneration through IL-6 and IL-8 autocrine signaling. Mol Immunol 2009;46:1374–86.
Liu Y, Kach A, Ziegler U, Ong AC, Wallace DP, Arcaro A, et al. The role of phospholipase D in modulating the MTOR signaling pathway in polycystic kidney disease. PLoS One 2013;8:e73173.
Mateos MV, Uranga RM, Salvador GA, Giusto NM. Activation of phosphatidylcholine signalling during oxidative stress in synaptic endings. Neurochem Int 2008;53:199–206.
Mateos MV, Salvador GA, Giusto NM. Selective localization of phosphatidylcholine-derived signaling in detergent-resistant membranes from synaptic endings. Biochim Biophys Acta 2010;1798:624–36.
Mateos MV, Giusto NM, Salvador GA. Distinctive roles of PLD signaling elicited by oxidative stress in synaptic endings from adult and aged rats. Biochim Biophys Acta 2012;1823:2136–48.
McDermott M, Wakelam MJ, Morris AJ. Phospholipase D. Biochem Cell Biol 2004;82:225–53.
Park SY, Cho JH, Ma W, Choi HJ, Han JS. Phospholipase D2 acts as an important regulator in LPS-induced nitric oxide synthesis in Raw 264.7 cells. Cell Signal 2010;22:619–28.
Peng X, Frohman MA. Mammalian phospholipase D physiological and pathological roles. Acta Physiol (Oxf) 2012;204:219–26.
Perez VL, Saeed AM, Tan Y, Urbieta M, Cruz-Guilloty F. The eye: a window to the soul of the immune system. J Autoimmun 2013;45:7–14.
Pollreisz A, Rafferty B, Kozarov E, Lalla E. Klebsiella pneumoniae induces an inflammatory response in human retinal-pigmented epithelial cells. Biochem Biophys Res Commun 2012;418:33–7.
Rodriguez DG, Uranga RM, Mateos MV, Giusto NM, Salvador GA. Differential participation of phospholipase A(2) isoforms during iron-induced retinal toxicity, Implications for age-related macular degeneration. Neurochem Int 2012;61:749–58.
Salvador GA, Giusto NM. Characterization of phospholipase D activity in bovine photoreceptor membranes. Lipids 1998;33:853–60.
Scott SA, Selvy PE, Buck JR, Cho HP, Criswell TL, Thomas AL, et al. Design of isoform-selective phospholipase D inhibitors that modulate cancer cell invasiveness. Nat Chem Biol 2009;5:108–17.
Sparrow JR, Hicks D, Hamel CP. The retinal pigment epithelium in health and disease. Curr Mol Med 2010;10:802–23.
Strauss O. The retinal pigment epithelium in visual function. Physiol Rev 2005;85:845–81.
Sung TC, Roper RL, Zhang Y, Rudge SA, Temel R, Hammond SM, et al. Mutagenesis of phospholipase D defines a superfamily including a *trans*-Golgi viral protein required for poxvirus pathogenicity. EMBO J 1997;16:4519–30.
Tarr JM, Kaul K, Chopra M, Kohner EM, Chibber R. Pathophysiology of diabetic retinopathy. ISRN Ophthalmol 2013;2013:343560.
Valledor AF, Comalada M, Xaus J, Celada A. The differential time-course of extracellular-regulated kinase activity correlates with the macrophage response toward proliferation or activation. J Biol Chem 2000;275:7403–9.
Viringipurampeer IA, Bashar AE, Gregory-Evans CY, Moritz OL, Gregory-Evans K. Targeting inflammation in emerging therapies for genetic retinal disease. Int J Inflam 2013;2013:581751.
Whitcup SM, Nussenblatt RB, Lightman SL, Hollander DA. Inflammation in retinal disease. Int J Inflam 2013a;2013:724648.
Whitcup SM, Sodhi A, Atkinson JP, Holers VM, Sinha D, Rohrer B, et al. The role of the immune response in age-related macular degeneration. Int J Inflam 2013b;2013:348092.
Zeng XX, Zheng X, Xiang Y, Cho HP, Jessen JR, Zhong TP, et al. Phospholipase D1 is required for angiogenesis of intersegmental blood vessels in zebrafish. Dev Biol 2009;328:363–76.
Zhang F, Zhao G, Dong Z. Phosphatidylcholine-specific phospholipase C and D in stimulation of RAW264.7 mouse macrophage-like cells by lipopolysaccharide. Int Immunopharmacol 2001;1:1375–84.